Soft-tissue Artefact Assessment and Compensation in Motion Analysis by Combining Motion Capture Data and Ultrasound Depth Measurements

Azadeh Rouhandeh and Chris Joslin
Systems and Computer Engineering, Carleton University, 1125 Colonel By, Ottawa, Canada

Keywords: Soft-tissue Artefacts, Soft-tissue Motion Capture, Hip Joint Centre Correction.

Abstract: Accurately determining the hip joint centre is a necessary component in biomechanical human motion analysis to measure skeletal parameters and describe human motion. The hip joint centre can be estimated using functional methods based on the relative motion of the femur to pelvis using reflective markers attached to the skin surface through an optical motion capture system; but this suffers inaccuracy due to the soft tissue artefact. A key objective in movement analysis is the assessment and correction of this artefact; in this case we present a non-invasive method to assess and reduce the soft tissue artefact effects using optical motion capture data and tissue thickness from ultrasound measurements during flexion, extension, and abduction of the hip joint. Results show that the displacement of markers is non-linear and larger in areas closer to the hip joint. The marker displacements are dependent on the movement type, being relatively larger in abduction movement. The quantification of soft tissue artefacts is used as a basis for a correction procedure for hip joint centre and minimizing effects. Results show that our method for soft tissue artefact assessment and minimization reduces the error in the functional hip joint centre approximately from 13-23mm to 7-14mm.

1 INTRODUCTION

Human hip joint is generally considered as a ball-and-socket joint that connects the hip bone and femur. The accurate location of the Hip Joint Centre (HJC) is a necessary component in functional analysis of the hip to measure skeletal parameters and describe human motions. The location of the hip joint can be estimated through various methods which can be divided into three categories: image-based techniques, predictive methods, and functional methods (Kirkwood et al., 1999; Leardini, 1999). Imaged-based determination of the hip centre requires a medical imaging modality such as x-ray radiographs, CT scans and magnetic resonance imaging (MRI). In these techniques, standardized images of the pelvis are obtained and the HJC location is considered as the geometrical centre of the head of the femur modeled as a circle in 2D images and a sphere in 3D images. One error in determination of HJC location using image-based techniques is caused by the assumption of the femoral head as a sphere although it is not perfectly spherical. The use of image-based determination of the HJC is limited as MRI-based techniques require expensive medical imaging and the other modalities in this category expose the subject to ionizing radiation (Speirs et al., 2012; Bell et al., 1989). Predictive methods estimate the HJC based on regression equations between palpable bony landmarks and the joint centre (Bell et al, 1989). These methods need the exact locations of bony landmarks in the calculations of HJC. The accuracy of them depends on identification of the anatomical landmarks and the error range of them in able-bodied adults was reported to be between 25-30mm (Camomilla et al., 2006). This error is higher in people with pelvic deformities due to the assumption of hip symmetry for both legs in these methods (Bouffard, 2012). The error associated with the predictive methods has led to an increased interest in identifying hip joint centres using the functional methods. Functional methods are based on the relative motion of the femur to the pelvis. In order to have the functional centre of the hip joint, the relative motion of the femur to the pelvis must be accurately measured. Optical motion capture systems are the

Rouhandeh, A. and Joslin, C.
Soft-tissue Artefact Assessment and Compensation in Motion Analysis by Combining Motion Capture Data and Ultrasound Depth Measurements.
DOI: 10.5220/0006624205110521
In *Proceedings of the 13th International Joint Conference on Computer Vision, Imaging and Computer Graphics Theory and Applications (VISIGRAPP 2018) - Volume 4: VISAPP*, pages 511-521
ISBN: 978-989-758-290-5

most used systems in the study of human movement which are non-invasive. In optical motion capture, reflective markers are attached to the skin of the body and cameras track 3D trajectories of the markers. In this technique of movement recording, the internal bone is inaccessible and markers are not rigidly placed on the bone; thus, there is the relative motion between the markers and bone due to muscles activities and skin deformation which is known as Soft Tissue Artefact (STA). One of the main objectives in human movement analysis is the assessment and correction of the soft tissue artefact, as it is the main source of error.

Several techniques have been presented to assess STA which are separated into five categories: intra-cortical pins, external fixators, percutaneous trackers, radiographic examinations, and magnetic resonance imaging (Leardini et al., 2005). Techniques based on intra-cortical pins, external fixators, and percutaneous trackers can represent relatively accurate measurements of the bone motion; but the use of these techniques is limited as the procedures of applying them are invasive and subjects may experience pain. The main drawbacks of techniques based on radiographic examinations are these methods are invasive due to radiation exposure, the 3D measurements of the STA are estimated from two planes which provide 2D information, and these techniques require extensive processing of image data (Sangeaux et al., 2006). MRI-based techniques require expensive medical imaging and they are not suitable for everyday clinical measurements and analyses (Yahia-Cherif et al., 2004).

Several methods have been proposed to reduce the STA effects: the solidification model, multiple anatomical landmark calibration, pliant surface modelling, dynamic anatomical landmark calibration, point cluster technique, global minimization, and techniques based on MRI (Leardini et al., 2005; Yahia-Cherif et al., 2004). The solidification model does not compensate the STA effects well as it can only identify erroneous frames (Leardini et al., 2005; Cheze et al, 1995). Dynamic calibration and multiple anatomical landmark calibration are based on invalid assumptions (linearity assumptions) and they are time consuming because they require additional data acquisitions (Cappello, 2005). The limitations of the point cluster technique are an overabundance of markers and instability (Alexander and Adriacchi, 2001; Ceratti et al., 2006). The drawback of the global optimization technique is that it simplifies joints structures that are not subject-specific which cannot be applied to people with hip joint disorders (Lu and O'Connor, 1999; Stagni et al., 2009). MRI-based techniques are expensive and consequently they are inappropriate for everyday clinical uses.

Despite the numerous methods proposed, the objective of a reliable non-invasive and clinical assessment and correction of STA in human hip joint kinematics is still being investigated, and this is the domain where our work lies in. We proposed a method for assessing STA using optical motion capture analysis and ultrasound depth measurements (UDM) (Rouhandeh et al., 2014a). To quantify STA, we processed the motion capture data using principal component analysis (PCA) to align the central axis of the bone in each movement type (Rouhandeh et al, 2014a). In this study, we present our mathematical method for assessing and correcting STA using optical motion capture analysis and ultrasound depth measurements based on finding three key markers, which is the basis for our previous study (Rouhandeh et al., 2014b).

2 MATERIALS

2.1 Overview

We propose a method consisting of ultrasound measurements of tissue thickness and motion capture analysis to quantify and minimize STA non-invasively to determine the HJC using a functional method. Our solution is to first record each marker's position placed on the thigh and pelvis for a range of motions of the hip joint (standing, flexion, extension, and abduction). When the thigh moves, the muscles of the upper thigh area contract and relax which cause change in the muscle thickness. These changes affect the positions of the markers attached to the skin relative to the underlying bone and introduce an STA error in the calculation of the HJC. We propose using ultrasound imaging to measure the changes in tissue thickness, UDM, at the marker positions for the same standing and extended positions. This information is used to select three markers having less change in their tissue thickness. These markers are considered as three key markers and will be further used in mathematical analysis on the data to assess and eliminate STA effects. Next step is fitting curves to the markers' positions and applying UDM information in order to determine bone positions at the positions of three key markers. In fact, by determining these positions, we eliminate the error in markers positions caused by changes in tissue thickness. We use these positions on the bone to assess STA during several movements of the hip joint as the. Therefore, once the bone positions at three key

markers of all motions of the hip joint (standing, flexion, extension, and abduction) have been determined, we attempt to find a rotation matrix and translation vector which transform the bone positions at three key markers of standing position to each of the other movement types as the bone is rigid body. By applying the matrix and the vector to the markers trajectories of standing position and comparing with the trajectories of markers of the other movement types, the STA can be quantified. The next step is the HJC calculation; we calculate the HJC using a coordinate transformation technique, SCoRE algorithm (Ehrig et al., 2006). In order to have an accurate HJC location, we use the displacement of the markers from the previous step and recalculate the markers' positions to eliminate STA effects used in the SCoRE algorithm. Our method is outlined in Figure 1 and each step is described in the following subsections.

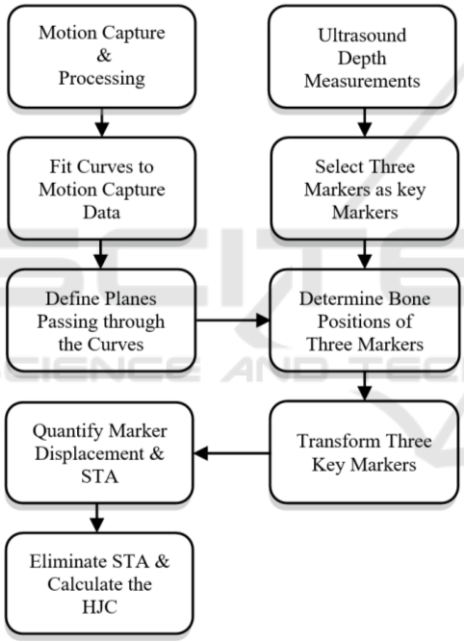

Figure 1: Overall Process for STA Assessment and Compensation.

2.2 Motion Capture

Ten healthy adult volunteers participated in this study after signing an informed consent. Optical motion capture systems are the most used systems in human movement studies. Our optical motion capture system is a Vicon MX system consisting of 10 wall-mounted near-infrared cameras. The subject is surrounded by the cameras while small reflective markers placed on the skin surface. To capture the movement of the hip joint, we use two groups of markers attached to the skin of the subjects. The first group of markers consists of 8 spherical reflective ones at palpable bony landmarks where the bone is very close to the skin surface and thus the soft tissue artefact is minimal. These locations include three on the hip area, left and right anterior superior iliac spine and the lower spine, two on either side of the knee, medial and lateral femoral epicondyles, and two on either side of the ankle, medial and lateral malleolus, and one on grater trochanter. As our goal is soft tissue artefact assessment in hip joint kinematics, the other group consists of the markers which are distributed over the skin of the thigh. These markers are affixed to the skin surface of the subjects in four ring formations. The rings are placed approximately 5cm apart, with eight markers per ring. These positions are marked on the thigh and used for the ultrasound depth measurements in the second stage of our experiments in this thesis. The markers configuration of the thigh is illustrated in Figure 2.

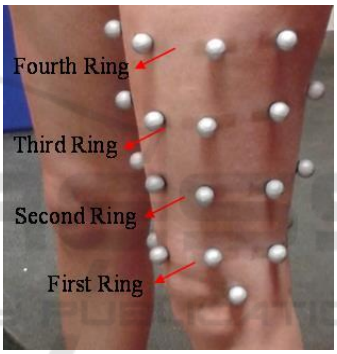

Figure 2: Subjects' Thigh Markers Configuration.

Once the markers have been attached to the subject's skin surface, we can capture and track the movements of the hip joint. The first step in our motion tracking is capturing the markers trajectories in standing position as a reference for subsequent processing. Participants are requested to move their leg which is equipped with the reflective markers in three key motions, flexion, extension, and abduction, starting from standing position. Markers trajectories are captured for these positions as shown in Figure 3.

To have the same range of motion of the hip joint for ultrasound depth measurements, the positions are determined using non-reflective blocks that are setup ahead of capture with a specific configured distance.

2.3 Ultrasound Measurements

There Ultrasound is one of the preferred imaging modalities because this modality is non-invasive and poses no harm to human bodies and, in addition, it is

a low cost and portable imaging modality. In our proposed method, to improve the determination of the HJC location, ultrasound imaging is used to measure the tissue thickness. Depth measurements were obtained using an ultrasound imaging machine (Picus, Esaote Europe) and a standard linear probe (L10-5, 5MHz operating frequency, 4cm wide).

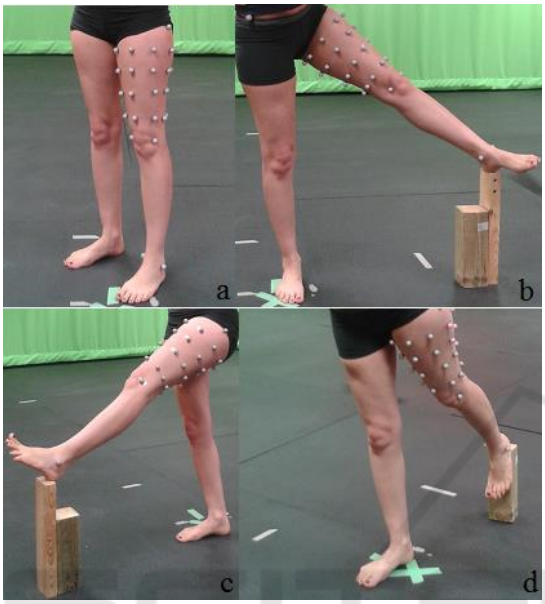

Figure 3: Subject Positions during Optical Motion Capture, a) Standing, b) Abduction, c) Flexion, and d) Extension

Using the ultrasound imaging to measure thickness of the tissue from the bone position, ultrasound echoes pass through tissues. As soft tissues and the underlying bone having different acoustic impedances, their reflected echoes are different. In fact, ultrasound echoes reflected from the bone surface are very strong and cause high intensity pixels in the image representing the bone surface. Detecting the desired edges in ultrasound images is not easy as they are extremely noisy and consist of various artefacts and unrelated high contrast noise.

In our application, the echoes reflected from the layered structures of different muscles cause relatively high intensity pixels and consequently error in detecting the desired bone surface. When we observe unrelated edges that make the bone surface detection difficult, we give a little push to the ultrasound probe to distinguish the unrelated edges. As mentioned, these unrelated edges are caused by the layered structures of different muscles; therefore, pushing the ultrasound probe changes the thickness of the muscles and structures of corresponding high intensity pixels in the image however the pixels correspond to the bone surface are not changed. After detecting the desired edge, the probe is released to measure the real thickness of soft tissues.

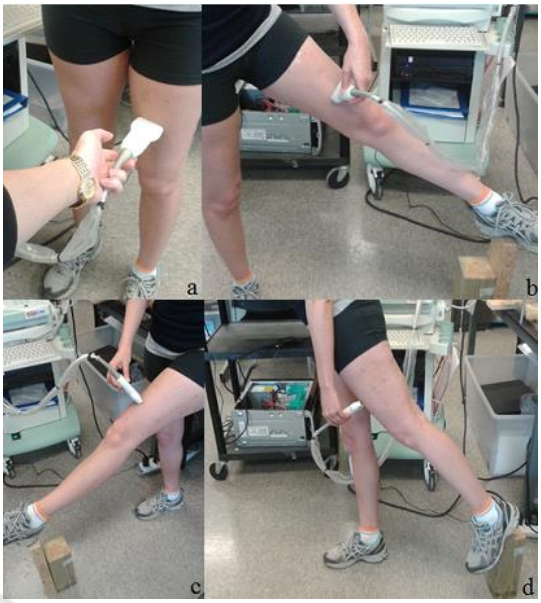

Figure 4: Subject Positions during Ultrasound Depth Measurements, a) Standing, b) Abduction, c) Flexion, and d) Extension.

3 DATA ANALYSIS & METHOD

3.1 Overview

In this section, we explain our proposed approach consisting of five steps to analyze data for STA assessment. The first step is finding three of the markers which have less depth changes during all positions (standing, flexion, extension, and abduction). The second step is passing a curve through the ring formation of each of the key markers. The third step is defining planes passing through the curves from the previous step. Then we propose a mathematical method to determine the projection of the key markers on the underlying bone. These positions on the bone are considered as references for the later processing in the STA assessment. All the steps are explained in detail in the following sections.

3.2 Determining Key Markers

Once the tissue thickness of the indicated markers on the thigh has been measured, we need to find three of the markers which have less depth changes during all positions (standing, flexion, extension, and abduction). To this aim, the coefficient of variation

(CV) of each marker's depth measurements during all positions is obtained and three markers with less value of CV will be selected as three key markers for next steps of our method. As the coefficient of variation measures relative variability and describe the variation relative to mean of a set of data, it is useful to compare data variation among two or more sets of data. The low value of the CV shows that the dispersion in the variable of a set of data is not great. The coefficient of variation of each marker is calculated using Equation (1).

$$CV = \frac{S}{\mu} \tag{1}$$

Where $S = \sum_{i=1}^{4}(D_i - \mu)^2/3$, $\mu = \sum_{i=1}^{4} D_i/4$ and D_i is the depth measurements for all four positions.

3.3 Curve Fitting

The next step is generating smooth curves which pass through the key data points of the ring formation of the motion capture data. To this end, we use a piecewise polynomial cubic spline interpolation. In piecewise polynomial cubic spline interpolation, a cubic polynomial is fitted between each pair of markers data of the ring formation to create a smooth curve. If we consider the markers data of motion capture, eight markers per each ring formation, are the sampled points from our desired curve, our goal is to find an approximated function between each consecutive pair of these eight points. For one dimension of the points, we have 8 distinct nodes x_i such that: $x_1, x_2, \dots, x_7, x_8$. Equation (2) gives the cubic polynomial in each subinterval to have a closed interpolated curve.

$$S(x) = \begin{cases} S_1(x), & x \in [x_1, x_2] \\ S_2(x), & x \in [x_2, x_3] \\ \vdots & \\ S_7(x), & x \in [x_7, x_8] \\ S_8(x), & x \in [x_8, x_1] \end{cases} \tag{2}$$

Where $S_i(x)$, as given by Equation (3), is a cubic polynomial that will be used on the subintervals.

$$S_i(x) = a_i x^3 + b_i x^2 + c_i x + d_i, \quad i = 1, \dots, 7, 8 \tag{3}$$

To define the spline, $S(x)$, four unknown parameters of each $S_i(x)$ should be found based on the interpolation conditions and continuity conditions in both the first and second derivatives which are expressed in Equation (4) and (5) for $i = 2, \dots, 7, 8$.

$$S_{i-1}(x_i) = S_i(x_i) \tag{4}$$

$$S'_{i-1}(x_i) = S'_i(x_i)$$
$$S''_{i-1}(x_i) = S''_i(x_i)$$

To have a closed curve, the cubic polynomial in subintervals $[x_1, x_2]$ and $[x_8, x_1]$, $S_1(x)$ and $S_8(x)$ should satisfy the following conditions in Equation (5).

$$S_8(x_1) = S_1(x_1)$$
$$S'_8(x_1) = S'_1(x_1) \tag{5}$$
$$S''_8(x_1) = S''_1(x_1)$$

By applying the conditions, the cubic polynomials in the subintervals and consequently $S(x)$ are determined. As cubic spline interpolation is continuous in both the first and second derivatives everywhere in subintervals and at the merging points, it is a useful interpolating method in our application to produce smooth interpolated functions.

3.4 Defining a Plane

To determine the bone position at the three key markers, we need to define a plane containing the bone which passes through each curve from the previous step. To define the plane, we need to provide three non-collinear points on the plane: one of the three key markers, P, one data point on the curve which is very close to the marker, Q, and one other marker data on the opposite side of the first marker data, R. Figure 5. shows these three points.

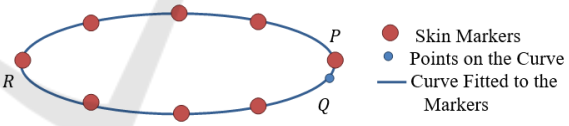

Figure 5: Passing a Plane through Each Curve.

The general equation of a plane is defined by Equation (6).

$$ax + by + cz + d = 0 \tag{6}$$

Given the coordinates of these three points in space, $P = [x_P, y_P, z_P]$, $Q = [x_Q, y_Q, z_Q]$, and $R = [x_R, y_R, z_R]$, we can find the parameters of the equation of the plane using Equation (7).

$$a = y_P(z_Q - z_R) + y_Q(z_R - z_P) + y_R(z_P - z_Q)$$
$$b = z_P(x_Q - x_R) + z_Q(x_R - x_P) + z_R(x_P - x_Q) \tag{7}$$
$$c = x_P(y_Q - y_R) + x_Q(y_R - y_P) + x_R(y_P - y_Q)$$

$$d = -x_P(y_Q z_R - y_R z_Q) - x_Q(y_R z_P - y_P z_R) - x_R(y_P z_Q - y_Q z_P)$$

3.5 Bone Position at Key Markers

Once the plane has been defined, we apply the ultrasound depth measurements at the positions of three key markers to determine three points on the bone. To determine these points on the bone, they should satisfy three conditions:

- This point should lie on the plane from the previous step
- The distance between the bone position and the key marker data on the position that the ultrasound depth is measured should be equal to the ultrasound depth measurement
- If we define two vectors, one between the key marker data and the data point on the curve which is very close to the marker and the other vector between the key marker data and the bone point, these two vectors should be perpendicular; as the UDM is the minimal distance between the skin surface and the bone.

Figure 6 illustrates the curve fitted to the markers' data and a point on the underlying bone at the position of one of the key markers.

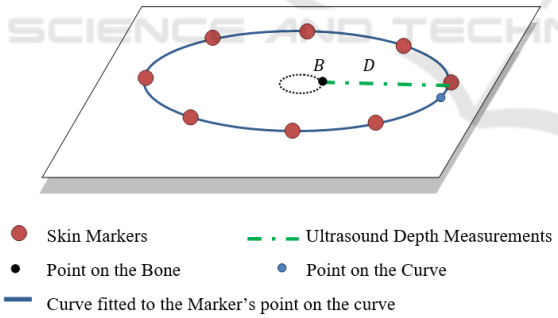

Figure 6: Determining Points on the Bone.

The conditions for the points on the femur bone can be written as Equations 8, 9 and 10, respectively. In the following equations, $B = [x_B, y_B, z_B]$ is the desired point on the bone and D is the ultrasound depth measurement. The coordinate of the bone point satisfies Equation (8) so that it is on the plane passing through the key marker point.

$$ax_B + by_B + cz_B + d = 0 \quad (8)$$

The distance between the bone position and the key marker which is equal to the ultrasound depth measurement is given by Equation (9).

$$D = \sqrt{(x_B - x_P)^2 + (y_B - y_p)^2 + (z_B - z_P)^2} \quad (9)$$

Vector PQ and PB are perpendicular if the dot product is equal to zero as given by Equation (10).

$$PQ.PB = (x_Q - x_P)(x_B - x_P) + (y_Q - y_p)(y_B - y_p) + (z_Q - z_P)(z_B - z_P) = 0 \quad (10)$$

3.6 Transformation of Key Markers

In the previous step, the bone positions at the three key markers of all movement types of the hip joint were determined. Determining these positions on the bone, the errors associated with the changes in tissue thickness at markers trajectories are eliminated; therefore, these bone positions are considered as data without the STA. By having these points, we can find a rotation matrix and a translation vector which transform the bone positions at the three key markers of the standing position to each of the other movements. We derive the matrix and vector by solving a linear least square problem recursively. Our objective function for each movement (compared with standing position) is given by Equation (11).

$$min_{\boldsymbol{R},t} \sum_{i=1}^{3} \|\boldsymbol{R}s_i + t - m_i\|^2 \quad (11)$$

Where $\boldsymbol{R}$ is the rotation matrix (3×3), t is the translation vector (3×1), s_i is the vector of key marker i in standing position (3×1), and m_i is the corresponding key marker of the other movements (3×1).

3.7 Quantification of Soft-tissue Artefact

The most important aspect of STA is to determine how the markers are displaced relative to the underlying bone due to the movement. Due to muscle contractions and skin deformation, markers move during different range of motions of the hip. We propose a method to determine three points on the bone which are the projection of positions of three markers having less change in their tissue thickness during all range of movements of the hip. We propose an approach to determine the transformation matrix and translation vector of the bone positions from the standing position to the other types of movements.

Determining the transformation matrix and translation vector, we have the rigid movement of the bone. If no STA error exists in the markers' trajectories, then they would move as rigidly as the bone. Therefore, to quantify STA, we apply the matrix and vector to the trajectories of the markers of standing position, compare with the trajectories of markers of the other movements, and compute the displacement of the markers.

3.8 Determining Hip Joint Centre

To determine the HJC, we use the SCoRE algorithm (Ehrig et al, 2006) which considers both joint segments, femur and pelvis, in the CoR estimation. In this algorithm, a local coordinate system for each moving segment of the joint (pelvis and femur head) is defined, and then these local systems for all time frames are transferred into a global reference system to estimate the HJC.

4 EXPERIMENTS AND RESULTS

4.1 Setup

The acquisition was performed at Carleton University's Motion Capture Studio and Ultrasound Imaging Laboratory. The study was carried out on 10 volunteers (5 females and 5 males) aged between 21 and 30 years (Mean: 27.2 years; Std. dev.: 2.7 years) with a mean body weight 64.1 (Std. Dev.: 13.9) of kg and a mean height 172.1cm (Std. Dev.: 8.7).

By processing the motion capture data using MATLAB and curve-fitting toolbox, we could fit the curves passing through the markers data and determine the bone positions at three key markers from the previous step.

Figure 7 illustrates the trajectories of all markers placed on the skin surface of one of the subjects during standing position in optical motion capture, the curves fitted to motion capture data, secondary points on the curves used in determination of the points on the bone, and the trajectories of key markers projections on the underlying bone.

After the determination of the bone positions at the three key markers, we used these locations as references and we found rotation matrices and translation vectors that transformed the bone positions at the three key markers of the standing position to each of the other movements, flexion, extension and abduction. We derived them by solving linear least square problems recursively in MATLAB. If the markers locations didn't suffer from soft tissue artefacts, they would have the same movement as the bone from standing to the other movement types. Based on this fact, we applied the rotation matrix and translation vector (corresponding to each movement) to the markers trajectories of standing position and compared with the trajectories

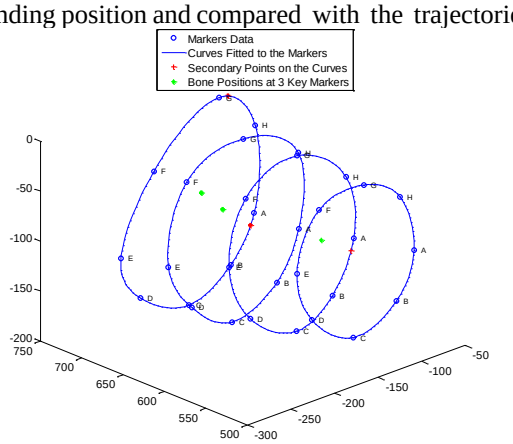

Figure 7: Curve Fitting to Motion Capture Data and Determination of Bone Positions at 3 Key Points Positions of Standing Position.

of markers of that corresponding movement, and then computed the displacement of the markers.

4.2 Trajectory Results

Figure 8 illustrates the trajectories of markers from optical motion capture which suffer from STA, and the corresponding trajectories after applying rotation matrix and translation vector to the markers trajectories of standing position to have data without STA effects. This figure shows the 3D displacements of the markers during abduction movement.

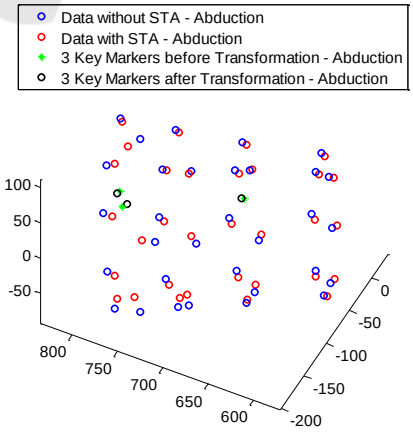

Figure 8: Transformation of Standing Markers to Abduction Movement.

4.3 Displacements Due to STA

As the study was carried out on 10 subjects, to show the results of the markers' displacements of all the subjects, we used box-plots. In the box-plot representation of markers displacements, the lowest value, highest value, median value, and the size of the first and third quartile of each marker displacement for all participants were illustrated. Figures 9, 10, 11, and 12 show the displacements of the markers of each ring during abduction movement.

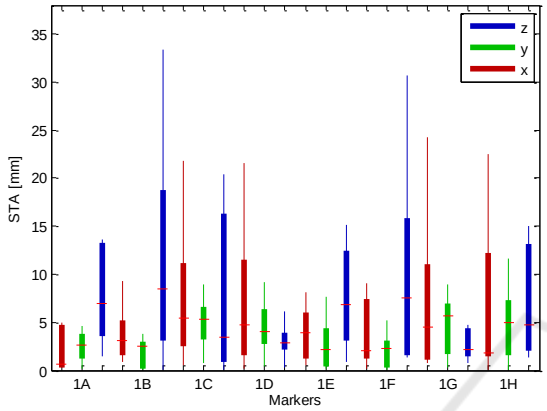

Figure 9: Box-plots of STA Components of the First Ring of Markers Configuration during Abduction.

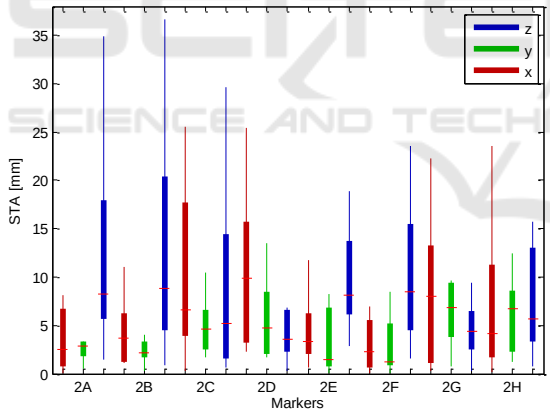

Figure 10: Box-plots of STA Components of the Second Ring of Markers Configuration during Abduction.

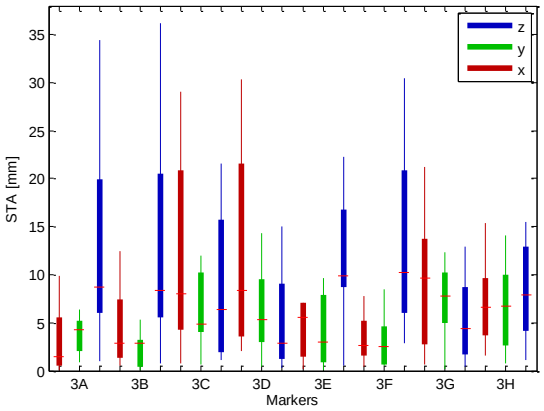

Figure 11: Box-plots of STA Components of the Third Ring of Markers Configuration during Abduction.

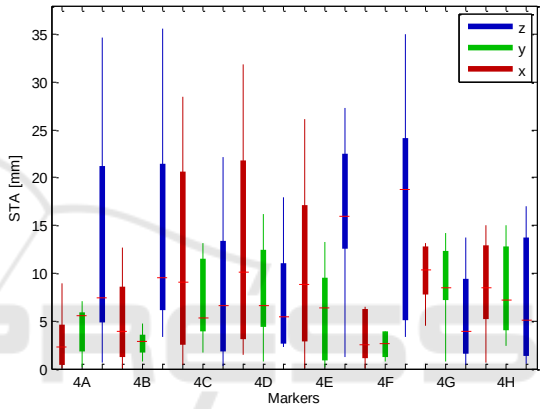

Figure 12: Box-plots of STA Components of the Fourth Ring of Markers Configuration during Abduction.

The assessment of STA was used to correct STA errors to more accurately determine the HJC location using the SCoRE algorithm. Two groups of markers consisting of three non-collinear markers were required to determine HJC using SCoRE algorithm, one group placed on the thigh and the other placed on the pelvis. As previously discussed, three key markers have less change in their corresponding tissue thickness during all movements; therefore, they were considered as the first group of markers attached to the thigh. The second group of markers included the trajectories of markers on the left and right anterior superior iliac spine and the lower spine. The second group of markers were placed on the bony landmarks and they were not affected by the STA. In this part, at first, we transferred all the markers in a way that the markers on the left and right anterior superior iliac spine and the lower spine match the same markers locations in the other movements. Then we applied the SCoRE algorithm (Ehrig et al., 2006) using Equation (12) on the 3 key markers, once on the markers positions before reducing STA and once

when we recalculated the markers positions (the positions on the bone) based on the STA quantification.

$$\begin{pmatrix} \boldsymbol{R}_1 & -\boldsymbol{S}_1 \\ \vdots & \vdots \\ \boldsymbol{R}_4 & -\boldsymbol{S}_4 \end{pmatrix} \begin{pmatrix} C_F \\ C_P \end{pmatrix} = \begin{pmatrix} d_1 - t_1 \\ \vdots \\ d_4 - t_4 \end{pmatrix} \quad (12)$$

Where C_F, C_P are the joint centres of the femoral and pelvic segments in the local coordinate systems, R_i, S_i are rotation matrices and t_i , d_i are translation vectors to transform the local coordinate systems of the pelvis and femur to an appropriate global system. We calculated $\boldsymbol{R}_1$,…, $\boldsymbol{R}_4$ and d_1,…, d_4 based on the markers attached to the thigh and $\boldsymbol{S}_1$,…, $\boldsymbol{S}_4$ and t_1,…, t_4 based on the markers attached to the pelvis as discussed before. The indices of these parameters indicate four frames that correspond to the frames of standing position, flexion, extension and abduction. For each participant during each movement, the SCoRE algorithm returned two centres and the distance between them showed the effectiveness of our method in minimizing STA effects (Ehrig et al., 2011).

4.4 Hip Joint Centre Error

Figures 13, 14, 15, and 16 show the error in determination of the hip joint centre for all subjects during standing position, flexion, extension and abduction. Each subject has two levels of error; one based on the markers positions before reducing STA and one based on the recalculated positions of the markers after eliminating STA.

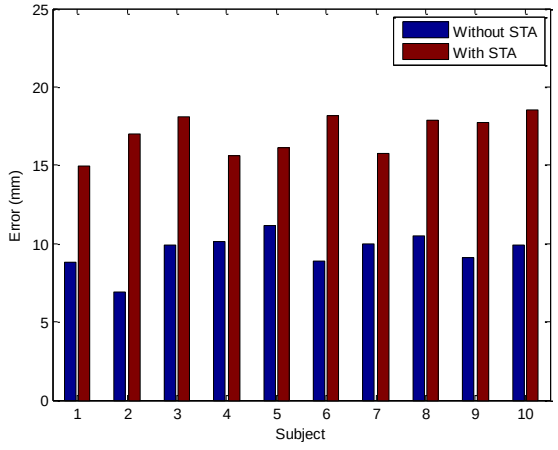

Figure 13: Hip Joint Centre Location Error Using SCoRE Algorithm, Standing Position.

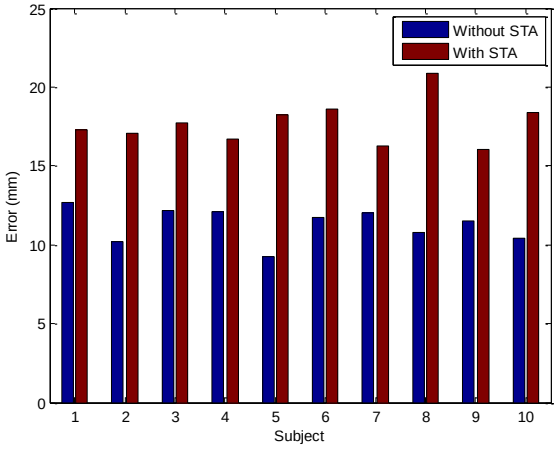

Figure 14: Hip Joint Centre Location Error Using SCoRE Algorithm, Flexion.

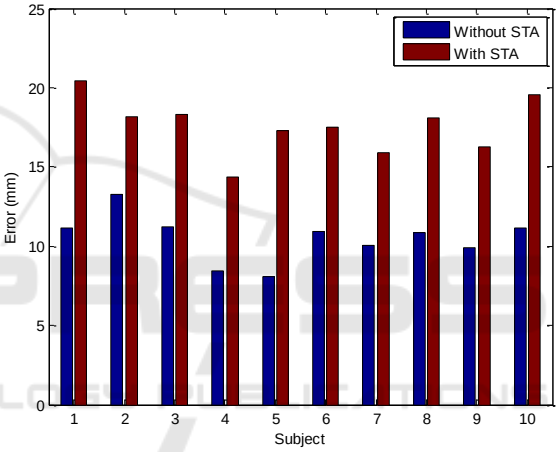

Figure 15: Hip Joint Centre Location Error Using SCoRE Algorithm, Extension.

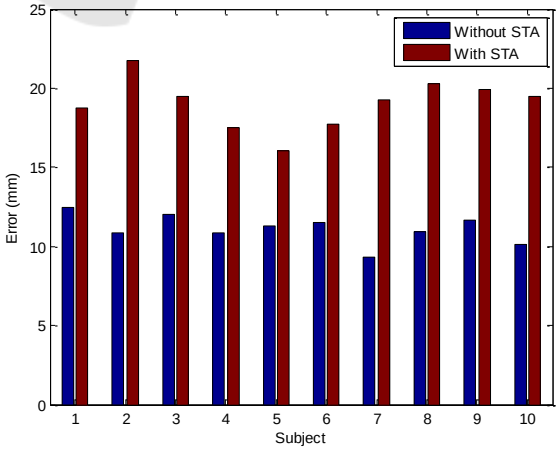

Figure 16: Hip Joint Centre Location Error Using SCoRE Algorithm, Abduction.

5 CONCLUSION

Soft tissue artefact is the most significant source of error in human movement analysis. In this study, we have proposed a combined experimental setup of optical motion capture system and ultrasound imaging system. The optical motion capture system is the most common used system in human movement studies as it tracks trajectories of the markers to have realistic motions of the body non-invasively. Ultrasound is one of the preferred imaging modalities because this modality is non-invasive and poses no harm to human bodies and, in addition, it is a low cost and portable imaging modality. As the optical motion capture system and ultrasound imaging system are non-invasive, our proposed experimental setup is non-invasive and appropriate for clinical daily uses in contrast to the previous studies on STA assessment and compensation which were invasive.

Using optical motion capture system along with ultrasound depth measurements data, we quantified STA on ten subjects during three ranges of motions of the hip joint, flexion, extension, and abduction comparing with natural position which was considered standing position. At first, we recorded each marker's position placed on the thigh and pelvis for a range of motions of the hip joint. We used ultrasound imaging to measure the changes in tissue thickness at the marker positions for the same standing and extended positions. Three markers were selected as three key markers based on the ultrasound depth measurements. Then we proposed using a piecewise polynomial cubic spline interpolation to fit curves to the markers' positions and applying UDM information to determine bone positions at the positions of three key markers. We used these positions on the bone to assess STA during several movements of the hip joint as the.

The results showed the markers' displacements were non-linear, subject and task dependent, and generally larger in areas closer to the hip joint. The hip is surrounded by several muscles linked to bones via tendons. These muscles provide the joint stability and control body movements. As different muscles of the hip and thigh produce different movements of the hip, the markers displacements are dependent on the movement. Most of the subjects had relatively larger STA in abduction movement; because different subjects had muscles with different levels of strength.

This STA assessment was used to correct STA errors to more accurately determination of the HJC location using the SCoRE algorithm. For each subject during each movement, two centres of rotation were obtained; one based on markers trajectories before minimizing the STA and one centre after minimizing the STA and recalculating markers trajectories. The error associated with the data before minimizing the STA and after minimizing the STA effects was approximately in the range of 13-23mm and 7-14mm, respectively. The results obtained from our proposed method shows improvements over previous studies reported at 15-26mm (Ehrig, 2011; Piazza, 2004).

ACKNOWLEDGEMENTS

The work in this paper was funded and supported by an NSERC Collaborative Health Research Project.

REFERENCES

Kirkwood, R. N., Culham, E. G., Costigan, P., 1999. Radiographic and Non-invasive Determination of the Hip Joint Center Location: Effect on Hip Joint Moments. *In Clinical Biomechanics, Vol. 14, No. 4, pp. 227-235*

Leardini, A., 1999. Validation of a Functional Method for the Estimation of Hip Joint Centre Location. *In Journal of Biomechanics, Vol. 32, No. 1, pp. 99-103*

Speirs, A. D., Benoit, D. L., Beaulieu, M. L., Lamontagne, M., Beaulé, P. E., 2012. The Accuracy of the Use of Functional Hip Motions on Localization of the Center of the Hip. *In Journal of Hospital for Special Surgery, Vol. 8, No. 3, pp. 192-197*

Bell, A. L., Brand, R. A., Pedersen, D. R., 1989. Prediction of Hip Joint Centre Location from External Landmarks. *In Human Movement Science, Vol. 8, No. 1, pp. 3-16*

Camomilla, V., Cereatti, A., Vannozzi, G., Cappozzo, A., 2006 An Optimized Protocol for Hip Joint Centre Determination Using the Functional Method. *In Journal of Biomechanics, Vol. 39, No. 6, pp. 1096-1106*

Bouffard, V., 2012. Hip Joint Center Localisation: A Biomechanical Application to Hip Arthroplasty Population. *In World Journal of Orthopedics, Vol. 3, No. 8, pp. 131*

Leardini, A., Chiari, L., Croce, U. D., Cappozzo, A., 2005, Human Movement Analysis Using Stereophotogrammetry: Part 3. Soft Tissue Artifact Assessment and Compensation. *In Gait & Posture, Vol. 21, No. 2, pp. 212-225*

Sangeux, M., Marin, F., Charleux, F., Dürselen, L., Ho Ba Tho, M. C., 2006. Quantification of the 3D Relative Movement of External Marker Sets vs. Bones Based on Magnetic Resonance Imaging. *In Clinical Biomechanics, Vol. 21, No. 9, pp. 984-991*

Yahia-Cherif, L., Gilles, B. Molet, T., Magnenat-Thalmann, N., 2004. Motion Capture and Visualization of the Hip Joint with Dynamic MRI and Optical Systems. *In Computer Animation and Virtual Worlds, Vol. 15, No. 3-4, pp. 377-385*

Cheze, L., Fregly, B. J., Dimnet, J., 1995. A Solidification Procedure to Facilitate Kinematic Analyses based on Video System Data. *In Journal of Biomechanics, Vol. 28, No. 7, pp. 879-884*

Cappello, A., Stagni, R., Fantozzi, S., Leardini, A., 2005. Soft Tissue Artifact Compensation in Knee Kinematics by Double Anatomical Landmark Calibration: Performance of a Novel Method during Selected Motor Tasks. *In IEEE Transactions on Biomedical Engineering, Vol. 52, No. 6, pp. 992-998*

Alexander E. J., Andriacchi, T. P., 2001. Correcting for Deformation in Skin-based Marker Systems. *In Journal of Biomechanics, vol. 34, no. 3, pp. 355-361*

Cereatti, A., Della Croce, U., Cappozzo, A., 2006. Reconstruction of Skeletal Movement Using Skin Markers: Comparative Assessment of Bone Pose Estimators. *In Journal of NeuroEngineering and Rehabilitation [Online], Vol. 3*

Lu, T. W., O'Connor, J. J., 1999. Bone Position Estimation from Skin Marker Co-ordinates Using Global Optimisation with Joint Constraints. *In Journal of Biomechanics, Vol. 32, No. 2, pp. 129-134*

Stagni, R., Fantozzi, S., Cappello, A., 2009, Double Calibration vs. Global Optimisation: Performance and Effectiveness for Clinical Application. *In Gait & Posture, Vol. 29, No. 1, pp. 119-122*

Rouhandeh, A., Joslin, C., Qu, Z. and Ono, Y., 2014a, August. Non-invasive Assessment of Soft-tissue Artefacts in Hip Joint Kinematics Using Motion Capture Data and Ultrasound Depth Measurements. *In Engineering in Medicine and Biology Society (EMBC), 36th Annual International Conference of the IEEE, pp. 4342-4345*

Rouhandeh, A., Joslin, C., Qu, Z., Ono, Y., 2014b. Soft-tissue Artefact Assessment and Compensation in Hip Joint Kinematics Using Motion Capture Data and Ultrasound Depth Measurements. *In International Conference on Biomedical Engineering and Systems, Prague*

Ehrig, R. M., Taylor, W. R., Duda, G. N., Heller, M. O., 2006. A Survey of Formal Methods for Determining the Centre of Rotation of Ball Joints. *In Journal of Biomechanics, Vol. 39, No. 15, pp. 2798-2809*

Ehrig, R. M., 2011. The SCoRE Residual: A Quality Index to Assess the Accuracy of Joint Estimations. *In Journal of Biomechanics, Vol. 44, No. 7, pp. 1400-1404*

Piazza, S., Erdemir, A., Okita, N., Cavanagh, P., 2004, Assessment of the Functional Method of Hip joint Center Location Subject to Reduced Range of Hip Motion. *In Journal of Biomechanics, Vol. 37, No. 3, pp. 349-356*